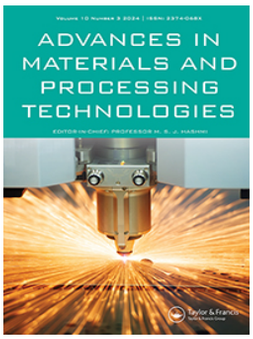

Advances in Materials and Processing Technologies

ISSN: (Print) (Online) Journal homepage: www.tandfonline.com/journals/tmpt20

Finite element method simulation of metal flow during Tubular Channel Angular Pressing (TCAP) of aluminium 7075

H Shagwira, JO Obiko & FM Mwema

To cite this article: H Shagwira, JO Obiko & FM Mwema (2024) Finite element method simulation of metal flow during Tubular Channel Angular Pressing (TCAP) of aluminium 7075, Advances in Materials and Processing Technologies, 10:3, 2460-2482, DOI: 10.1080/2374068X.2023.2216403

To link to this article: https://doi.org/10.1080/2374068X.2023.2216403

ADVANCES IN MATERIALS AND PROCESSING TECHNOLOGIES
2024, VOL. 10, NO. 3, 2460–2482
https://doi.org/10.1080/2374068X.2023.2216403

Finite element method simulation of metal flow during Tubular Channel Angular Pressing (TCAP) of aluminium 7075

H Shagwira[a], JO Obiko[b,c] and FM Mwema[d]

[a]Department of Mechanical and Industrial Engineering, Masinde Muliro University of Science and Technology, Kakamega, Kenya; [b]Department of Mining, Materials and Petroleum Engineering, Jomo Kenyatta University of Agriculture & Technology, Nairobi, Kenya; [c]School of Chemical and Metallurgical Engineering, University of Witwatersrand, Johannesburg, South Africa; [d]Department of Mechanical Engineering Science, University of Johannesburg, Johannesburg, South Africa

ABSTRACT

Tubular Channel Angular Pressing (TCAP) is among the upcoming and highly interesting, severe plastic deformation methods (SPD). This technique is reported to be appropriate for the deformation of very large strains in cylindrical tubes. The tube is pressed by a top die in a space between a mandrel and a die containing three shear zones while maintaining the same tube thickness and diameters. To investigate the SPD process in tubular samples, a commercially available pure aluminium alloy (AA7075) was used to evaluate the influence of die geometry, coefficient of friction, pressing speed, die temperature and tube thickness. The average grain size of about 500 nm was attained from 25 µm by extensive grain refinement. The results of Finite Element (FE) indicated that an effective strain of 3 was achieved by correctly choosing the input parameters. The thickness and length of the tube processed by TCAP also exhibited excellent strain homogeneity. The TCAP process can impose large strains because of having three deformation zones. Depending on input parameters selection, this SPD method, therefore, has two major advantages; (i) excellent strain homogeneity and (ii) high effective strain.

ARTICLE HISTORY
Accepted 16 May 2023

KEYWORDS
Finite element method; tubular channel angular pressing; severe plastic deformation; damage; load; effective stress; effective strain

1. Introduction

In the past decade, the Tubular Channel Angular Pressing (TCAP) technique has attracted much research interest and has been experimentally carried out and reported by several authors [1–5]. Figure 1 illustrates the TCAP die geometry, and as shown, the workpiece is positioned in the space formed between the mandrel and bottom die. Similarly, a top die which is a hollow cylinder having the same thickness as the workpiece is then positioned in the same space formed between the bottom die and the mandrel with its bottom surface in contact with the top surface of the workpiece. The top die presses the workpiece until it passes through three axisymmetric shear zones at the bottom die geometry. The tube thickness remains the same, while the TCAP process is

CONTACT H Shagwira hshagwira@mmust.ac.ke Department of Mechanical and Industrial Engineering, Masinde Muliro University of Science and Technology, Kakamega, Kenya

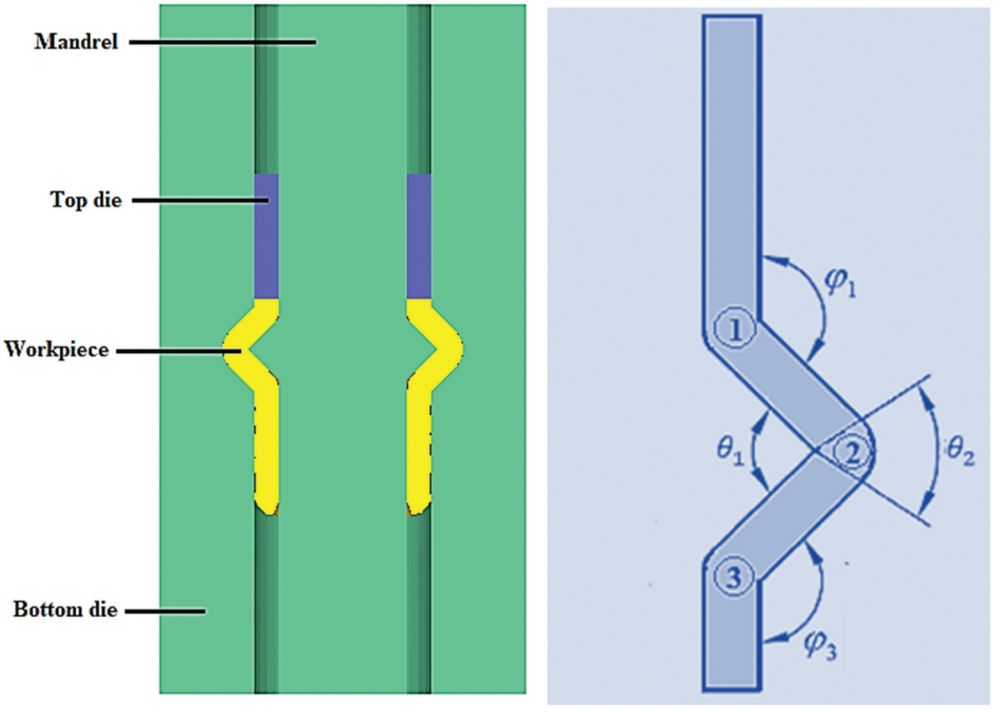

Figure 1. The TCAP die geometry with the three deformation regions 1, 2 and 3 and the die angles θ_1 and θ_2.

repeated as much as possible to exert the required effective strain on the tubular material [6].

The workpiece is severely deformed during the TCAP process to produce an ultra-fine grained (UFG) material. The existence of excess dislocations is critical in the enhancement of the UFG structure [7]. Studies have shown that the dislocation densities occurring during severe deformation play a key factor in determining the mechanical properties of the deformed metal [8]. Although the presence of high dislocation densities has an impact on the production of UFG materials, estimating the dislocation density is important [9,10]. The dislocation density can be determined with the Nix-Gao model or using transmission electron microscope (TEM) micrographs [5].

In this paper, the effects of die geometry, pressing speed, coefficient of friction, pressing force and die temperature on the effective strain, pressing load, damage and effective stress were studied. The objective was to investigate how each input parameter affects the dislocation density, hence work hardening. Work hardening in forming processes helps in improving the strength of the materials. The dislocations densities in SPD processes are usually too high hence large strains are achieved with UFG material produced [11]. Therefore, this paper provides an understanding of the concepts and ideas behind the achievement of UFG in tubular materials.

2. Methodology

As shown in Figure 1, the workpiece is in between the mandrel, and the bottom die. The top die has an internal and external diameter as the workpiece. The mandrel at the centre of the bottom die allows the initial tube thickness to be maintained. Therefore, the cylindrical space between the mandrel and the bottom die helps in keeping a constant tube thickness as it shears three times at the deformation regions 1, 2 and 3. During plastic deformation, the tubular workpiece experiences circumferential tensile, compressive, and shear deformation in a single pass during the TCAP process.

A commercial DEFORM 3D® software was used for FEM simulations of the TCAP process. Computer-aided design (CAD) software SOLIDWORKS® 2019 was used to design the die geometries and the tubular workpiece and imported into DEFORM 3D as STL file format. The material used in the workpiece was an alloy of Aluminium 7075 (AA7075) with the following material properties:

Young's Modulus	68900 MPa
Flow stress model	$\bar{\sigma} = \bar{\sigma}\left(\bar{\varepsilon}, \dot{\bar{\varepsilon}}, T\right)$
Yield function type	Von Mises
Hardening rule	Isotropic
Poisson's ratio	0.3
Thermal conductivity	180.175 W/mK
Emissivity	0.7

The workpiece had the dimensions of an internal diameter of 25.4 mm, a thickness of 2.5 mm, and a length of 40 mm. The dies were assumed to be rigid so that they could not undergo any plastic deformation. The workpiece was meshed up to 32,000 elements while applying the Lagrangian incremental for smooth emulation of the actual TCAP process. The TCAP process temperature was 25 °C. A maximum die displacement of 40 mm was chosen as a stopping criterion. The direct iteration method was a preferred iteration technique that shortens the simulation time. A friction coefficient of 0.05 was selected, which corresponds to MoS_2 lubricant, used mostly for experimental tests. The heat transfer coefficient was 45 N/sec/mm/°C. During workpiece pressing, a top die moving at a speed of 5 mm/sec was used. The simulation set-up is, as shown in Figure 2.

Microstructural evolution was modelled using Avrami's model. The equation of Avrami describes the transformation of solids from one phase to another while maintaining a constant temperature. This equation is therefore very important in crystallisation kinetics. Dynamic recrystallisation was used. Dynamic recrystallisation occurs when the strain-induced tend to exceed critical strain during deformation.

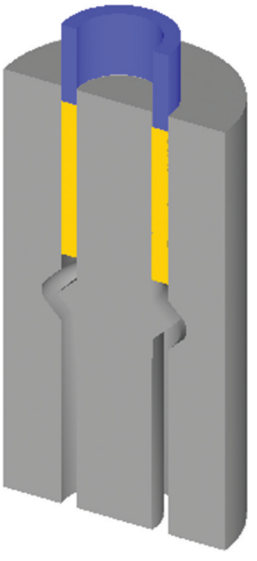

Figure 2. A sliced TCAP set-up showing the workpiece, top die, bottom die and the mandrel.

3. Results and discussion

3.1. Microstructural evolution

The microstructural evolution of Aluminium 7075 with a face-centred cubic (FCC) crystal structure and atomic radius of 0.1431 nm was modelled to observe the process of SPD in achieving a nanostructure. The FCC has a slip plane of type {111} with a direction ⟨110⟩. The burger's vector for FCC crystal structure for metals is expressed as

$$\mathbf{b}(\mathrm{FCC}) = \frac{\mathrm{a}}{2}\langle 110\rangle$$

where *aisunitcelledgelength* and is expressed as $a = 2R\sqrt{2}$ and *Ristheatomicradius*.

For Aluminium 7075,

$$\begin{aligned} \mathrm{a} &= 2 \times 0.1431\sqrt{2} \\ &= 0.4047nm \end{aligned}$$

The magnitude of the burger's vector is given by;

$$|\mathrm{b}| = \frac{\mathrm{a}}{2}\sqrt{\mathrm{u}^2 + \mathrm{v}^2 + \mathrm{w}^2} \tag{1}$$

where u, v, w are the components of the burger's vector for FCC crystal structure for metals.

To model the microstructural evolution, it is necessary to calculate the magnitude of the burger's vector, which is calculated using Equation 1.

$$|\mathrm{b}| = \frac{0.4047}{2}\sqrt{1^2 + 1^2 + 0^2}$$

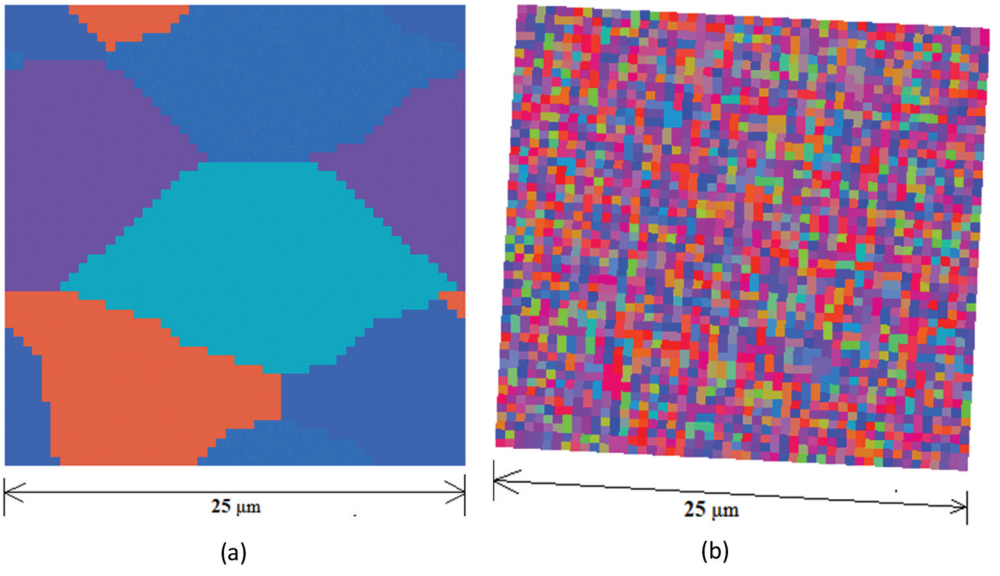

Figure 3. The microstructural evolution during the TCAP process with (a) at the start of pressing and (b) at the end of pressing.

$$|b| = 0.2862\,nm$$

Figure 3 shows the microstructural evolution during the TCAP process with (a) before pressing and (b) after pressing. The results show that the TCAP process can refine AA7075 grains to nano-size. From the results, the average size of the grains of 25 μm was reduced to about 500 nm. This implies that there is an increase in strength and strain in the material.

3.2. Influence of die geometry

3.2.1. Variation in θ_1

3.2.1.1. Effective strain. Strain value represents the deformation degree that occurs in the material during deformation. There are two slightly different types of strains commonly used: true strain and engineering strain. The true strain used commonly for large plastic deformation analysis, such as TCAP in DEFORM 3D simulations. Engineering strain is the change in length of a material divided by its initial length and it is widely used in most engineering applications (Equation 2).

$$Engineering\ strain = \frac{\Delta\ Change\ in\ length}{Original\ length} \tag{2}$$

Engineering strain is appropriate when deformations are small, but starts to break down when large deformations are involved. It is preferable to adopt true strain for large plastic deformation analysis. The true strain can be described as the sum of arbitrarily many small increments of strains that are integrated over the total change in length (Equation 3).

$$\in = \ln \frac{l_f}{l_0} \tag{3}$$

where ϵis the true strain, $l_f is$ the final length and $l_0 is$ the initial length

The effective strain is associated with the yielding process during plastic deformation. The effective strain is a component of the true strain that grows monotonically when deformation goes beyond the yielding limit. The effect of the effective strain on the workpiece was studied using the following die geometries: $\theta_1 = 70°, 90°, 110°, 120° and 130°$.

Figure 4 shows the distribution of effective strain along the length and across the thickness of the workpiece. The study shows that using angles $\theta_1 > 90°$ resulted in a lower effective strain of less than 3, but with a homogeneous effective strain distribution along the length and across the thickness of the workpiece. Lower strains achieved when $\theta_1 > 90°$ are attributed to low dislocation densities at this region, and hence elongation tends to impose large strains are limited.

3.2.1.2. Pressing load. Figure 5 shows the load versus time flow curves at different die geometries during deformation. The flow curves showed that the deformation load increased with a decrease in die angle θ_1. A maximum deformation load of 450 kN (70°), while the lowest deformation load of 190 kN (130°). The variation in the pressing load results from an increase in back-pressure that tends to resist material flow, thus a large force is required to overcome the back-pressure. It is desirable to use the lowest deformation load possible in the TCAP process. The deformation load curves for 110°, 120° and 130° channels had relatively smooth curves, an indication of lower compressive stresses.

3.2.1.3. Damage. Damage typically indicates the possibility of ductile fracture occurring in a workpiece material. In FEM, the exact description of damage depends on the preprocessor's calculation technique. Based on the model chosen from the material library in the FEM pre-processor, a damage factor describes the damage that occurs at each element. In metal forming processes, the likelihood of the formation of a fracture can well be predicted using the damage factor. As the workpiece deforms, the damage factor tends to increase. Usually, fracture occurs when the critical value has been exceeded. Damage does not provide an indicator of tool fracture in metal forming processes. Usually, die failure analysis is carried out using the stress component. However, since dies were assumed to be rigid, damage to the tool was not analysed in this study. In this study, the damage analysis was carried out using;

$$\int^{\bar{\varepsilon}} \sigma^* d\bar{\varepsilon} \tag{4}$$

where $\sigma^* is the maximum principal stress$ and $\bar{\varepsilon} is the effective strain$

Equation 4 is the Cockcroft-Latham model. This model has proven to be a good predictor for some forms of tensile-ductile fracture, that is, cracking as a result of deformation occurring due to stretching like chevron or surface cracking experienced in extruded materials. The critical damage factor for the fracture to start differs considerably from one material to another. The fracture behaviour depends on the material processing route. Nonetheless, the critical damage factor where the fracture occurs is generally repeatable for a particular material having a specific annealing treatment. The option

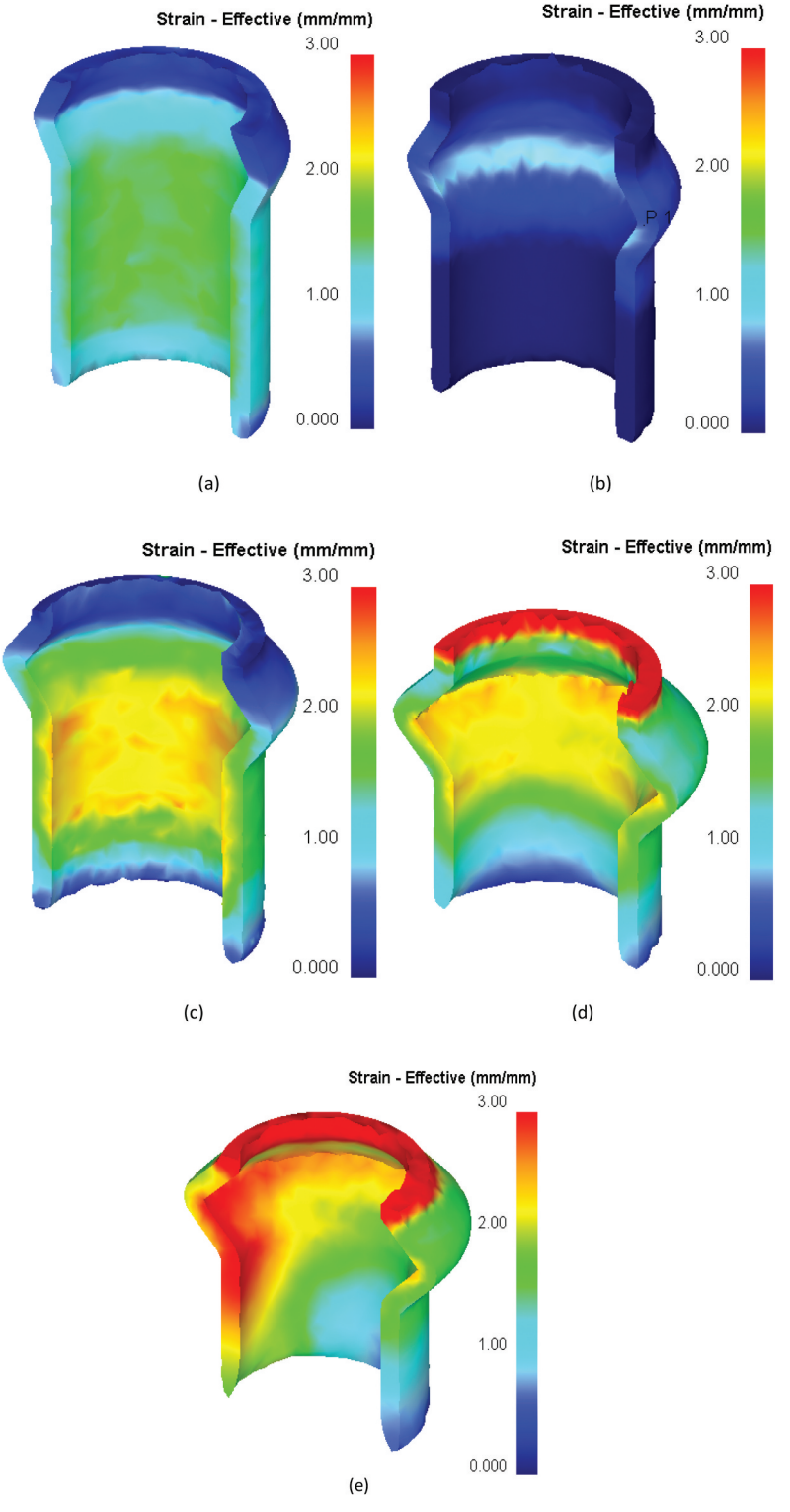

Figure 4. The distribution of effective strain along the length and across the thickness of the workpiece for θ_1 (a)130° (b) 120° (c) 110° (d) 90° and (e) 70°.

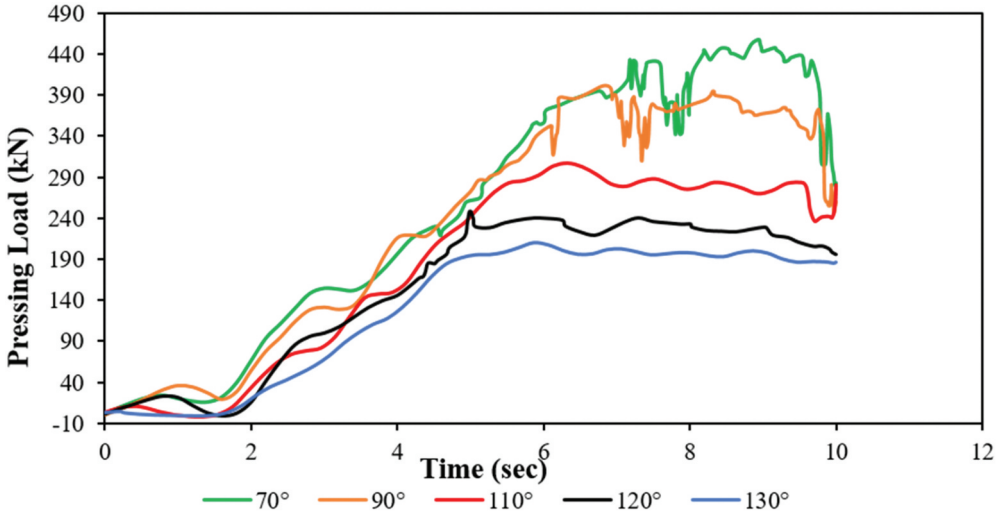

Figure 5. The pressing load variations in different die geometries during deformation.

with the lowest damage factor is the best option for reducing the probability of a fracture occurring in a workpiece during deformation simulations in FEM.

Figure 6 shows the variation in damage during deformation using different dies geometries. The damage curves show that die geometries having $\theta_1 \leq 90^\circ$ have high damage values than the ones having $\theta_1 > 90^\circ$. Damage value depicts the formation of fracture in a sample, using a small θ_1 increases the chance of the sample cracking during the TCAP processing. Since each of the element in the material undergoes a stepwise pattern of strain increments, the incremental strain rate in each element is higher for die geometries having $\theta_1 \leq 90^\circ$ as compared to die geometries having $\theta_1 > 90^\circ$. This incremental strain rate is attributed to a smooth strain rise over the deformation zone in die

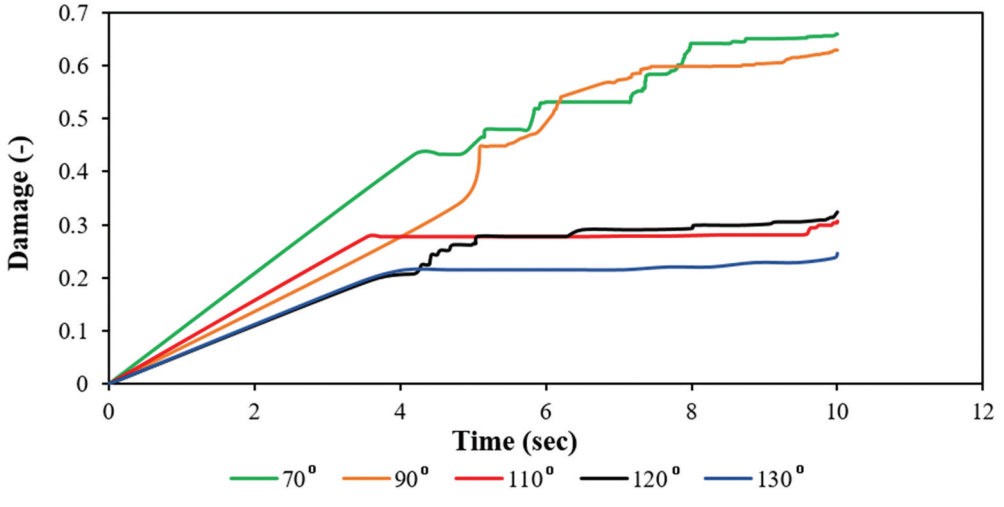

Figure 6. The damage imposed by different die geometries on the workpiece during deformation.

geometries having $\theta_1 > 90°$. Therefore, to avoid fracture of the material, $\theta_1 > 90°$ is recommended. It can be observed that $\theta_1 = 130°$ has the least damage value.

3.2.1.3.1. Variation in θ_2.

Effective strain.

It has been reported that round corners along the channels are likely to improve the lubrication of the outlet channel and reduce the pressing load [12]. Figure 7 shows effective strain distribution along the length and thickness of the workpiece.

The angles used in this study were $\theta_2 = 30°, 50°, 70°, 90° and 110°$. It is observed that 50° achieved a higher strain distribution of more than 3. A good strain distribution was observed in sample processed in dies having $\theta_2 = 110°$. This flow behaviour was attributed to the smooth flowability at the fillet. To reduce plastic overloading in region 2, the angle θ_2 should be greater than 45°. Uniform friction in both sides of the channels results in accumulated shear γ: composed by γ_1 along the inner radius, γ_2 along the outer radius, and γ_3 along the middle of the thickness. The distribution of γ shows strong non-uniformity extended through a large part of the cross-section of the material especially in $\theta_2 = 50°$. Generally, die geometries having sharp corners contain extend plastic zone which reduces strain, develops a dead metal zone, cause strain non-uniformity, redistribute shear between a few directions and modify the simple shear deformation mode. These changes are undesirable for structure formation and should be avoided or minimised.

3.2.1.4. Pressing load. Figure 8 shows the variation in pressing load with time while varying the die angle θ_2. It is observed that all the samples exhibited the same amount of pressing load with a maximum pressing load of about 400 kN attained. This implies that θ_2 has little or no effect on the backpressure. Its main role is in work hardening and ensuring the material achieves high strains and strength.

3.2.1.5. Damage. Figure 9 shows the variation of damage with θ_2. It is observed that a high likelihood of damage is achieved in the die geometry having $\theta_2 = 50°$. However, a damage value of less than 0.5 is only achieved in the die geometry of $\theta_2 = 110°$. This is attributed to the smooth shearing in AA7075 during the TCAP process, and the tendency of flow localisation and shear fracture to occur is resisted. These fractures usually form in regions experiencing high strain rates, that is, region 1, 2 and 3. Since the inner diameter experiences high strains than the outer diameter, there is a high chance of cracks forming in the inner zone than the outer zone of the tube. The die angle θ_2 directly affects the inner diameter of the workpiece. It is also observed that the damage increases as the workpiece deformation increases in all cases. The damage value from Cockcroft and Latham model relates to the effective strain. This is why an increase in the effective strain rate increases the damage value.

3.3. Influence of the coefficient of friction

Friction affects the plastic deformation process such as TCAP. When setting up this TCAP process, a tolerance of 0.0002 mm was used, and there is no full contact between material and channel. The friction conditions in the inner channel walls are much more

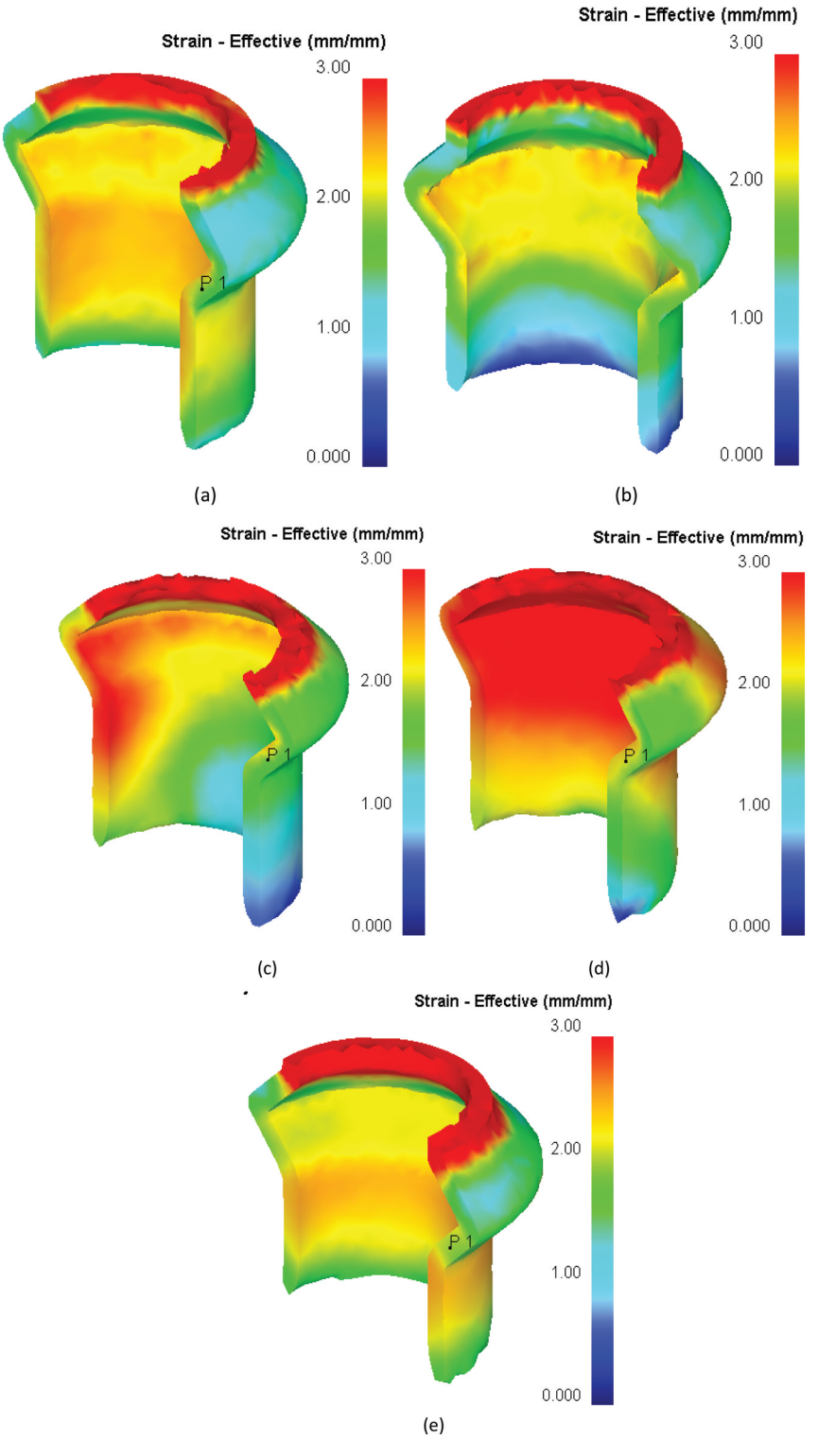

Figure 7. The distribution of effective strain along the length and across the thickness of the workpiece for θ_2 (a)110° (b)90° (c) 70° (d) 50° (e) 30°.

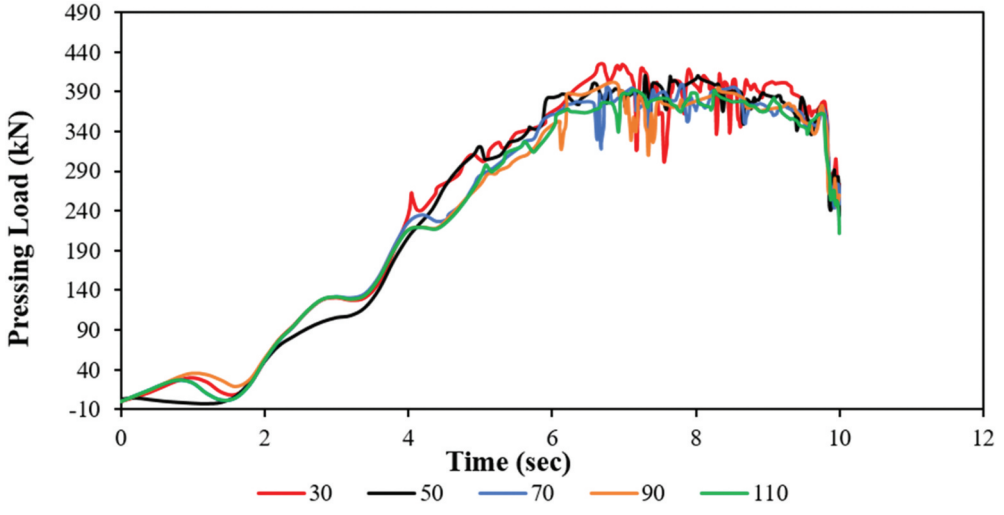

Figure 8. The pressing load variations in different die geometries(θ_2) during deformation.

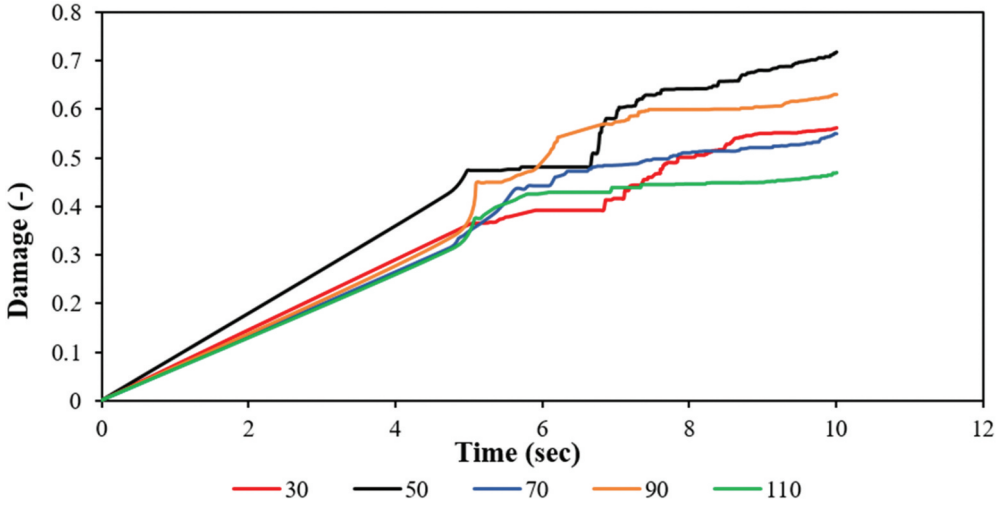

Figure 9. The damage variations with different die geometries (θ_2) during TCAP deformation.

favourable than those in the outer channel walls because the contact pressure at the channel walls is significantly lower and there is no dead metal zone. The lubricant is deposited directly on the workpiece and the channel. A thick grease with powder graphite and MoS_2 provides lubrication at cold and warm temperatures for TCAP processing [13,14].

Figure 10 shows the effective strain distribution in the workpieces. It is observed that high friction coefficients of 0.4 and 0.3 have much lower effective strain as compared to that of 0.2, 0.1 and 0.05. They additionally have damaged the top part implying that there was a lot of resistance to flow and high back-pressure. In all the cases apart from $\mu = 0.5$, there is a non-homogeneous

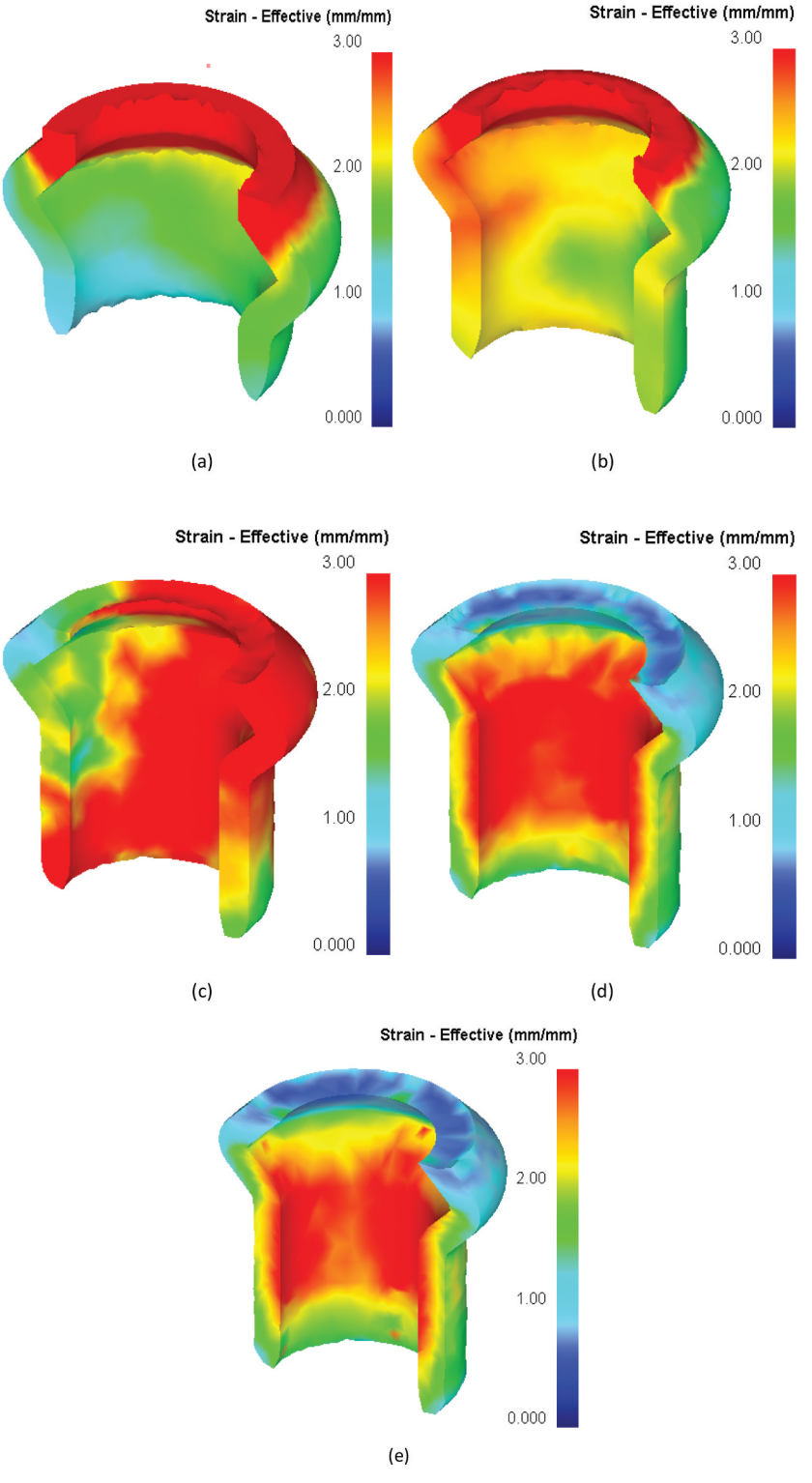

Figure 10. The distribution of effective strain along the length and across the thickness of the workpiece for friction coefficients of (a) 0.4 (b) 0.3 (c) 0.2 (d) 0.1 and (e) 0.05.

distribution of effective strain across the thickness of the tube. To avoid damage to the workpiece and achievement of high strains, it is therefore recommended to use a friction coefficient of less than 0.1.

3.4. Influence of the pressing speed

Considering the influence of pressing speed on the TCAP variables, a friction coefficient of 0.05 was used throughout as per the recommendation in section 3.3.

3.4.1. Strain

Figure 11 shows the effective strain distribution cross the thickness and along the length of the workpieces. It is observed that the pressing speed of 25 mm/sec had the highest strain attained at about 3. The effective strain homogeneity across the thickness of the workpieces was achieved for a pressing speed of 50 mm/sec. This is attributed to a high strain rate which is almost similar for all the elements across the thickness. It is also observed that damage at the top part of the workpieces was high in samples processed by 10 mm/sec, 25 mm/sec, 35 mm/sec and 50 mm/sec. This is attributed to the fact that high processing speeds tend to cause back pressure that causes resistance to the flow of the material.

3.4.2. Load

Figure 12 shows the variation in pressing load with time at varying pressing speed. In all the sample, a maximum pressing load of about 400 kN was achieved. This result shows that the pressing speed of less than 50 mm/sec has little effect on the maximum pressing load. However, higher strain rate results in structural defects, high dislocation density and internal stresses, hence cause cracking during TCAP.

3.4.3. Damage

As previously discussed, damage value predicts the likelihood of a fracture occurring in the workpiece. Therefore, the lower the damage value shows a better the deformation process. Figure 13 shows the variation of damage value during TCAP at different pressing speeds of 5 mm/sec, 10 mm/sec, 25 mm/sec, 35 mm/sec and 50 mm/sec. It is observed that using a pressing speed of greater than 25 mm/sec results in a high damage value as compared to 5 mm/sec and 10 mm/sec pressing speeds. The high damage values observed at speeds of 25 mm/sec, 35 mm/sec and 50 mm/sec are attributed to a high strain rate imposed on the workpiece material, which causes structural defects and internal stresses. During deformation, work hardening tends to reduce the damage that can occur in a workpiece [15]. Higher speeds affect mechanical properties such as the strength negatively and increase elongation [16]. There is limited work hardening at lower speeds, hence no fracture occurs.

3.5. Influence of the die temperature

3.5.1. Effective strain

Figure 14 shows the influence of the TCAP temperature on the effective strain distribution along the length, and across the thickness of the deformed sample. All the samples

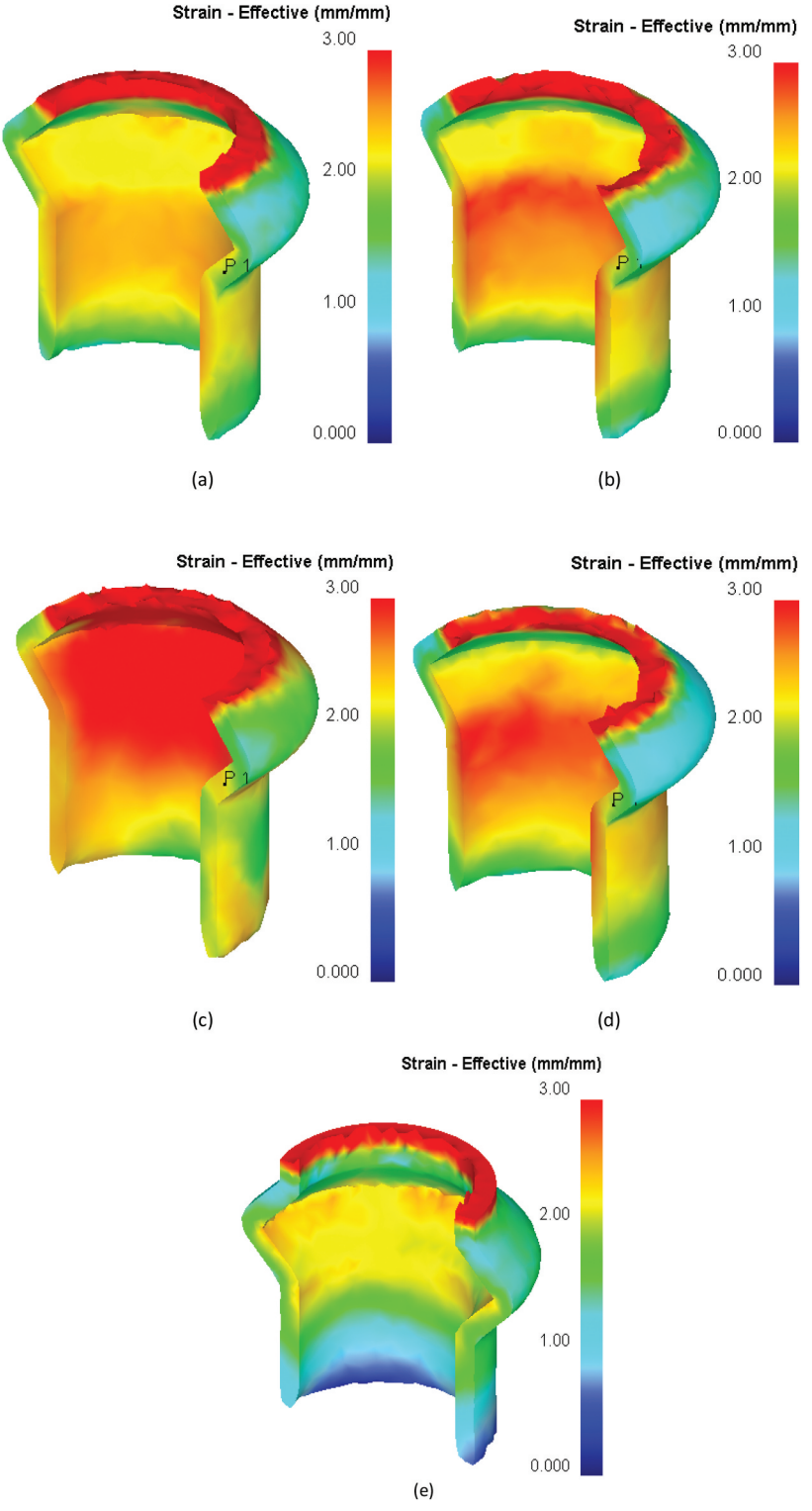

Figure 11. The distribution of effective strain along the length and across the thickness of the workpiece at different pressing speeds with (a) 50mm/sec (b) 35mm/sec (c) 25mm/sec (d) 10mm/sec and (d) 5mm/sec.

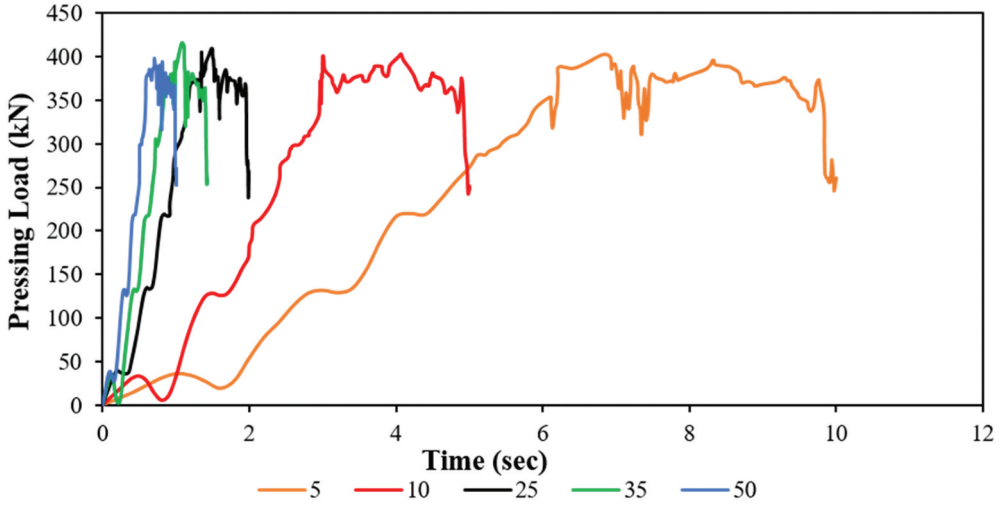

Figure 12. The pressing load variations during deformation for various pressing speeds in mm/sec.

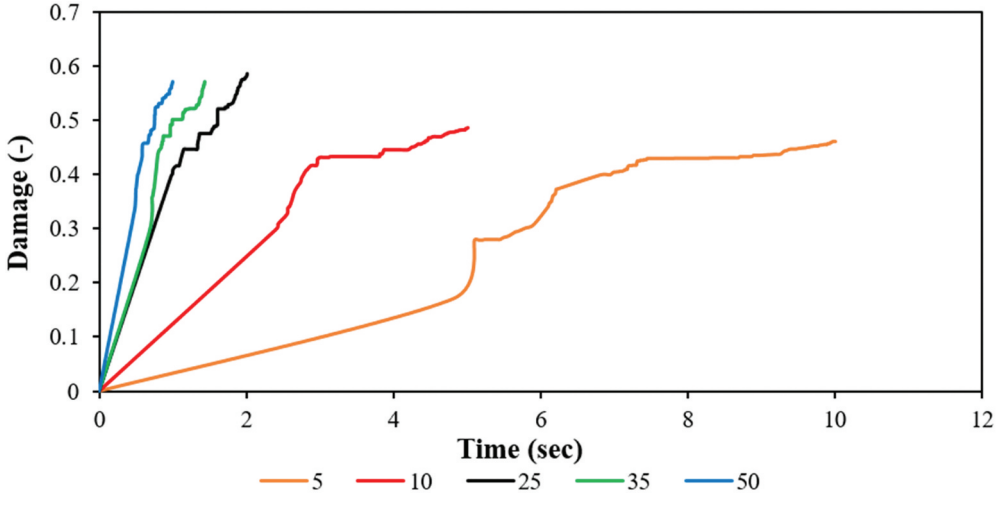

Figure 13. The damage variations during deformation for various pressing speeds in mm/sec.

exhibited homogeneous effective strain distribution across the sample thickness and along the length of the workpiece. A maximum effective strain of about 2.3 was achieved after processing. However, the top part of all the samples was damaged due to the backpressure during processing. Therefore, in conclusion, temperatures less than 500 °C do not affect the strain distribution in a workpiece processed by TCAP.

3.5.2. Pressing load

Figure 15 shows the variation in pressing load with time at various die temperatures. All the samples had a maximum pressing load of about 400 kN. This flow behaviour implies that there is high resistance to flow due to backpressure. The

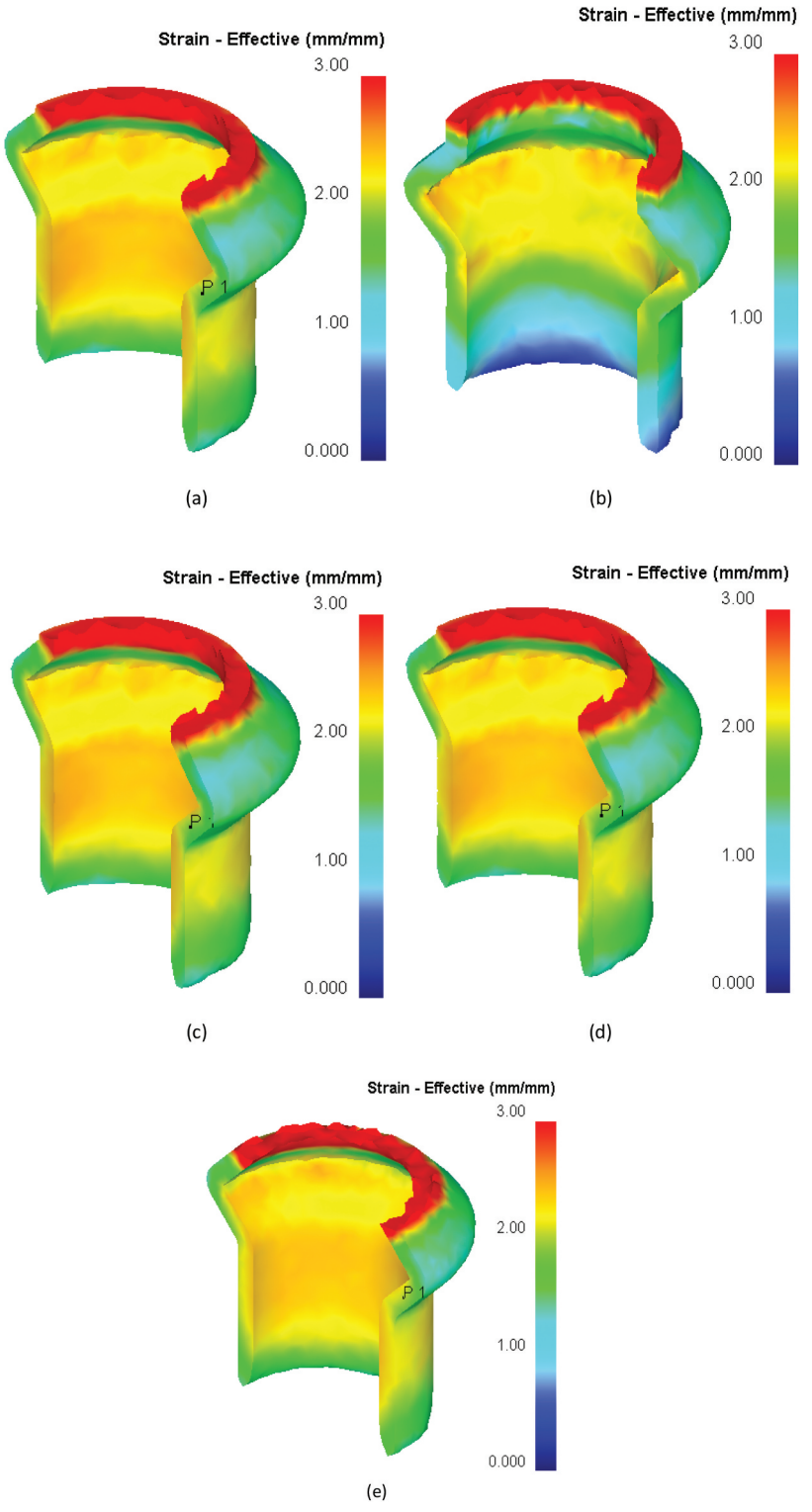

Figure 14. The distribution of effective strain along the length and across the thickness of the workpiece at different temperatures with (a) 500 °C (b) 300 °C (c) 200 °C (d) 100 °C and (e) 25 °C.

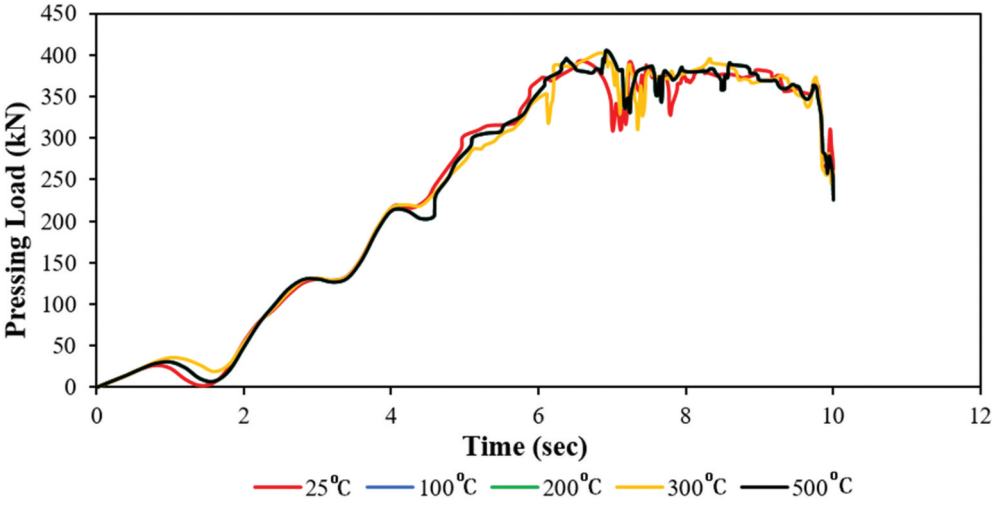

Figure 15. The pressing load variations versus time during deformation for various processing temperatures.

high resistance to metal flow may be the cause of the damage caused on the top part of the workpieces as observed in Figure 14 since the material tries to find an escape route even through the smallest gap possible. It was observed that all the TCAP processed had the same amount of pressing load. It can, therefore, be concluded that temperatures less than 500°C do not influence the pressing load during TCAP.

3.5.3. Damage

Figure 16 shows damage variation on the deformed workpiece at different die temperature. The results showed that the damage value was constant for all simulation tests. However, the damage value for 100 °C, 200 °C, and 500 °C overlap each other and have a maximum of about 0.45. The temperature of 300°C exhibited the highest damage value of 0.6. Since a lower damage value is desirable, it is recommended that temperatures of 100 °C, 200 °C, and 500 °C are suitable for TCAP processing.

3.6. Influence of the tube thickness

3.6.1. Strain

The sample thickness plays a role during the TCAP process by influencing the metal flow stress, and the deformation force. This, in turn, results in variation in mechanical properties in the tubes having different thickness. To demonstrate this, a TCAP die geometry of $\theta_1 = 90°$, $\theta_2 = 90°$ and $d_0 = 25.4mm$ were studied. A pressing speed of 5 mm/sec, the friction coefficient of 0.05, and the die temperature of 25were applied. The thicknesses of the tubes simulated were 2.5 mm, 3.2 mm, 4 mm and 5.5 mm. Comparisons on the effective strain/stress distribution, the pressing load, and the damage variations were analysed.

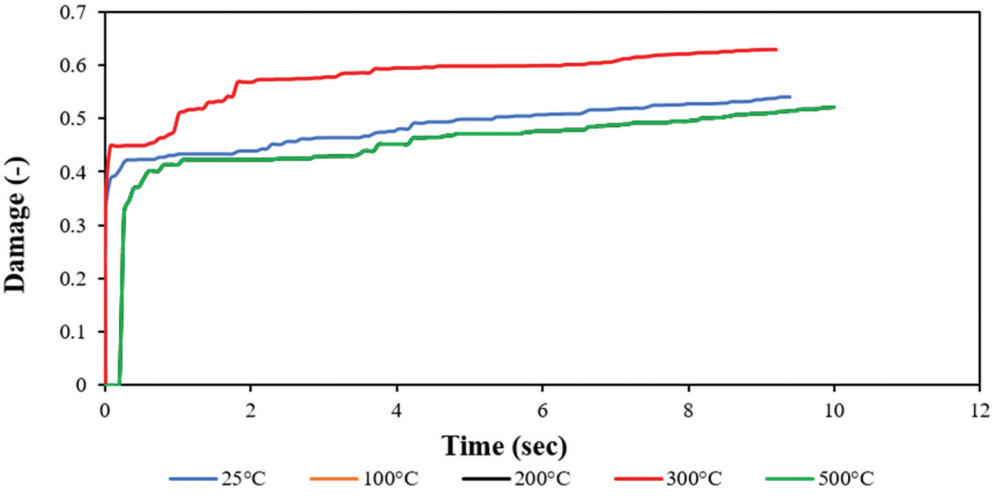

Figure 16. The damage variations during TCAP deformation of AA7075 at various processing temperatures.

Figure 17 shows the effective strain distribution along the length and thickness of the workpiece of 5.5 mm, 4 mm, 3.2 mm and 2.5 mm respectively. It is observed that the workpiece having 3.2 mm thickness had a homogeneous strain distribution of about 3 across its length as compared to that of 2.5 mm, 4 mm and 5.5 mm thickness. Even dislocation densities across the circumference of the tube will cause even flow stresses and hence even effective strains. However, there is uneven effective strain distribution across the thickness in all the cases. High effective strains occurred in the inside diameter as compared to the outside diameter. This is attributed to large double plastic deformations of the inner tube regions at zone 1 and 3 in the die geometry shown in Figure 1. The SPD process results in a finer grain in the inside regions than the outside region hence making the tubes stronger on the inside and such tubes can find application in transporting pressurised fluids. Additionally, higher effective strains occurred at the top layer of the workpiece having 2.5 mm thickness. The top part of the sample was damaged, as a result of contact between the die and the workpiece. Interfacial contact between the die and the workpiece results in high flow stress, hence causing damage. High flow stress may induce cracks or plastic separation of the deformed material due to circumferential strains. It has been reported that using a die with an inclined surface rather than a flat surface will guarantee that the deformed material retains its cohesion especially when small thickness tubes are deformed [17,18]. It has been found that the correct deformation conditions can be obtained by using hyperbolic dies rather than dies flat surfaces [19,20].

3.6.2. Pressing load

Figure 18 shows the variations in the pressing loads required to achieve UFG for each tubular workpiece. It is observed that the amount of pressing load increases with an increase in the thickness of the workpiece. This is because an increase in thickness increases the effective contact area between the die and the workpiece. To achieve the

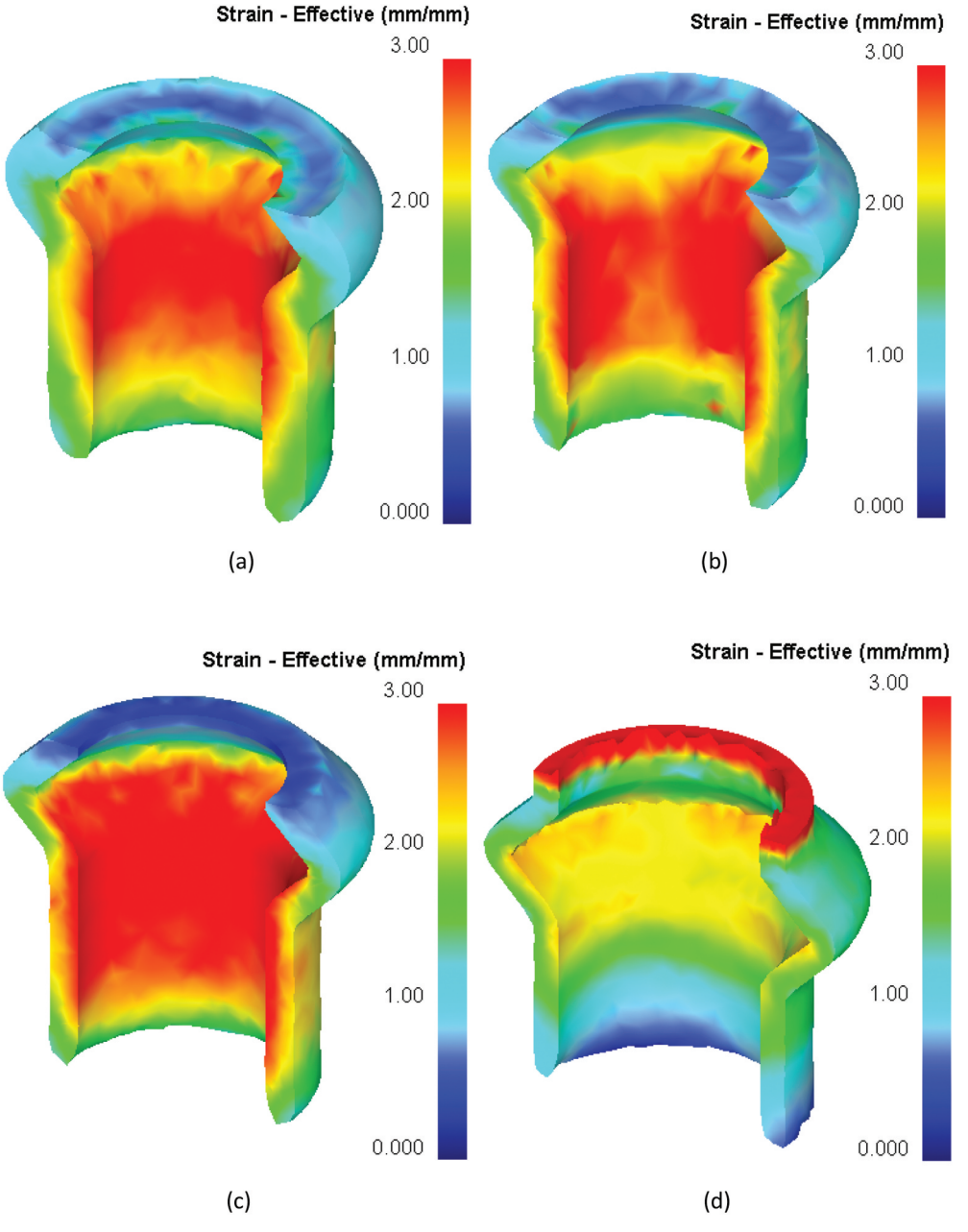

Figure 17. The distribution of effective strain along the length and across the thickness of the workpiece with (a) 5.5 mm (b) 4 mm (c) 3.2 mm and (d) 2.5 mm.

same effective stress, in all the samples means the pressing load has to increase. The maximum pressing load for various tube thickness were: 850 kN (5.5 mm), 600 kN (4 mm), 500 kN (3.2 mm), and 400 kN (2.5 mm). Figure 19 shows that there is a linear relationship between the maximum pressing load and the thickness of the tube.

The maximum pressing load can be predicted as

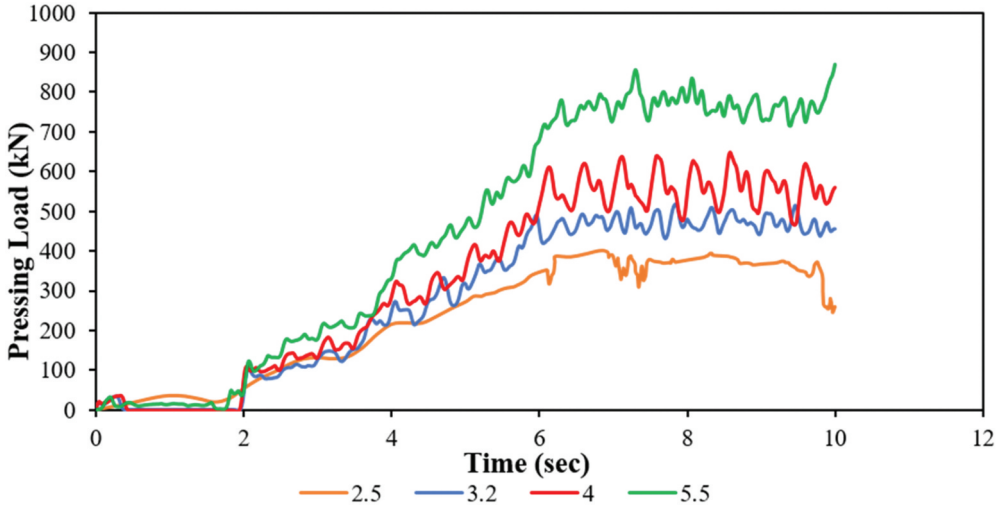

Figure 18. The pressing load variations with time during deformation for various workpiece thickness (mm).

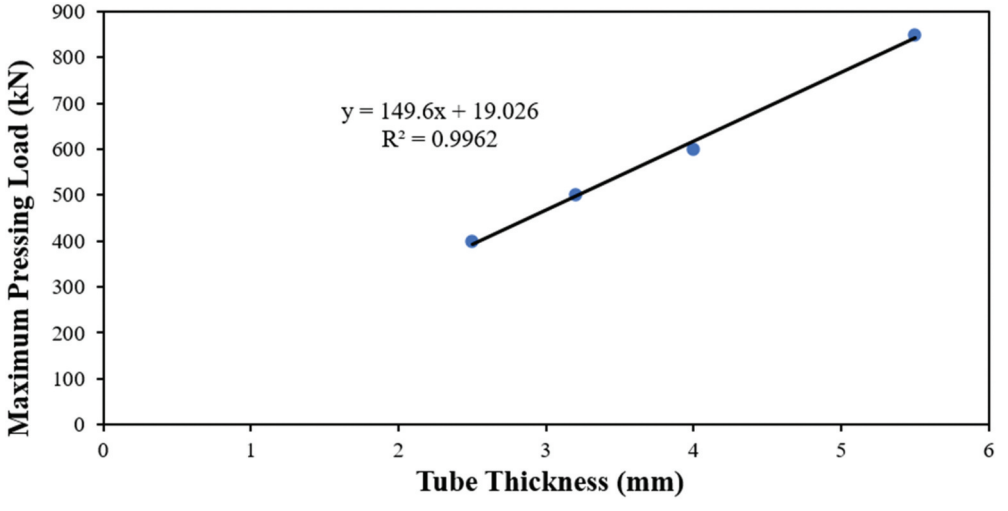

Figure 19. A relationship between the maximum pressing load and the thickness of the tube. It can be seen the two parameters exhibit a linear relationship with a very high correlation coefficient (R^2=0.9962).

$$y = 149.6x + 19.026 \tag{5}$$

where $yisMaximumPressingLoad(kN)$ and $xistubethickness(mm)$
Therefore, for an AA7075 tube with an internal diameter of $d_0 = 25.4mm$, it is possible to predict the maximum pressing load for the given tube thickness using Equation 7.

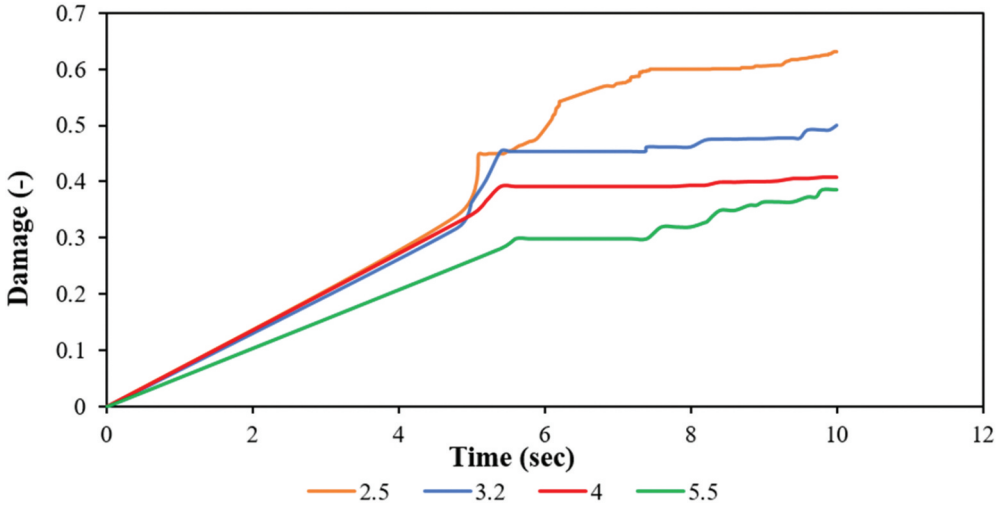

Figure 20. The variations in damage on the workpiece during deformation for different workpiece thickness.

3.6.3. Damage

Figure 20 shows the variation of damage at the same selected point in all the workpieces having different tube thickness. It is observed that damage increases with a decrease in tube thickness. The tube having a thickness of 2.5 mm experienced high damage at a maximum of 0.6 with the thickest tube of 5.5 mm having the least likelihood of damage at a maximum of 0.35. This observation is attributed to the variation in the contact area between the workpiece and the die. In the case where the contact area is small, the active surfaces of the die do not restrict the plastic flow and cracking hence damage of the AA7075 alloy becomes inevitable. This can be avoided by increasing the working area of the die by using hyperbolic dies rather than a flat surface dies [19,20].

4. Industrial implications and future directions

TCAP process has shown some promising future application because of its micro-forming ability. In the micro-forming process, parts are produced with their dimensions measuring from microns to millimetres. Micro-forming has the potential of becoming the world's most preferred metal forming process in the manufacturing industry due to its potential for mass production of small products while achieving a high surface finish, high production rate, and a low cost of production. Micro-formed tubes through TCAP can find good application in micro-vessels, bioengineering where micro-implants replace clogged blood vessels in hypertensive patients [21].

5. Conclusions

The factors affecting the TCAP process, i.e. the influence of die geometry, coefficient of friction, pressing speed, the die temperature and tube thickness were investigated on aluminium alloy (AA7075). After TCAP processing;

(a) the average grain size was reduced from 25 μm to about 500 nm through extensive grain refinement.
(b) the results of FEM showed that an effective strain of 3 could be achieved by the correct choice of the input parameters.
(c) the thickness and length of the tube processed by TCAP also exhibited excellent strain homogeneity except when parameters such as coefficient of friction are varied.
(d) generally, TCAP can impose large strains because it has three deformation zones (denoted as 1, 2, and 3 in this paper).

Therefore, the TCAP process is important because; (i) it can produce samples with excellent strain homogeneity and (ii) with very high effective strains.

Disclosure statement

No potential conflict of interest was reported by the authors.

ORCID

H Shagwira http://orcid.org/0000-0002-1115-932X

References

[1] Mwema FM, Matthew K, Harisson S, et al. Design optimization of angular extrusion for severe plastic deformation of tubular specimens. Int J Mech Appl. 2017;7:1–13.
[2] Faraji G, Ebrahimi M, Bushroa AR. Ultrasonic assisted tubular channel angular pressing process. Mater Sci Eng A. 2014;599:10–15.
[3] Faraji G, Mashhadi MM, Bushroa AR, et al. TEM analysis and determination of dislocation densities in nanostructured copper tube produced via parallel tubular channel angular pressing process. Mater Sci Eng A. 2013;563:193–198.
[4] Faraji G, Yavari P, Aghdamifar S, et al. Mechanical anD microstructural properties of ultra-fine grained AZ91 magnesium alloy tubes processed via multi pass Tubular Channel Angular Pressing (TCAP). J Mater Sci Technol. 2014;30(2):134–138.
[5] Faraji G, Babaei A, Mashhadi MM, et al. Parallel tubular channel angular pressing (PTCAP) as a new severe plastic deformation method for cylindrical tubes. Mater Lett. 2012;77:82–85.
[6] Mesbah M, Faraji G, Bushroa AR. Characterization of nanostructured pure aluminum tubes produced by tubular channel angular pressing (TCAP). Mater Sci Eng A. 2014;590:289–294.
[7] Zhao X, Li S, Zhang Z, et al. Comparisons of microstructure homogeneity, texture and mechanical properties of AZ80 magnesium alloy fabricated by annular channel angular extrusion and backward extrusion. J Magnesium Alloys. 2020;8(3):624–639.
[8] Jafarlou DM, Zalnezhad E, Hassan MA, et al. Severe plastic deformation of tubular AA 6061 via equal channel angular pressing. Mater Design. 2016;90:1124–1135.
[9] Kim K, Kang W, Lee S-I, et al. Microstructural evolution and enhancement of mechanical properties of Al1050 by tubular channel angular extrusion. Mater Sci Eng A. 2017;696:26–32.
[10] Tavakkoli V, Afrasiab M, Faraji G, et al. Severe mechanical anisotropy of high-strength ultrafine grained Cu–Zn tubes processed by parallel tubular channel angular pressing (PTCAP). Mater Sci Eng A. 2015;625:50–55.
[11] Ebrahimi M, Shaeri MH, Naseri R, et al. Equal channel angular extrusion for tube configuration of Al-Zn-Mg-Cu alloy. Mater Sci Eng A. 2018;731:569–576.

[12] Iwahashi Y, Wang J, Horita Z, et al. Principle of equal-channel angular pressing for the processing of ultra-fine grained materials. Scripta Materialia. 1996;35(2):143–146.
[13] Alimirzaloo V, Nikzad B, Ahmadi S, et al. Effect oF lubricant and operation temperature on the metallurgical property of AM60 magnesium alloy in ECAP process. Tribol Trans. 2019;62(5):821–827.
[14] Nagasekhar AV, Chakkingal U, Venugopal P. Candidature of equal channel angular pressing for processing of tubular commercial purity-titanium. J Mater Process Technol. 2006;173(1):53–60.
[15] Lowe TC, Valiev RZ. Investigations and applications of severe plastic deformation. Dordrecht, Netherlands: Springer; 2000.
[16] Li W-J, Deng K-K, Zhang X, et al. Effect of ultra-slow extrusion speed on the microstructure and mechanical properties of Mg-4Zn-0.5Ca alloy. Mater Sci Eng A. 2016;677:367–375.
[17] Faraji G, Mashhadi MM, Kim HS. Tubular channel angular pressing (TCAP) as a novel severe plastic deformation method for cylindrical tubes. Mater Lett. 2011;65(19–20):3009–3012.
[18] Frint P, Härtel M, Selbmann R, et al. Microstructural evolution during severe plastic deformation by gradation extrusion. Metals. 2018;8(2):96. DOI:10.3390/met8020096
[19] Faraji G, Kim HS, Kashi HT. Severe plastic deformation: methods, processing and properties/Ghader Faraji, H.S. Kim, Hessam Torabzadeh Kashi. Amsterdam: Elsevier; 2018.
[20] Zehetbauer M, Valiev RZ. *Nanomaterials by severe plastic deformation: proceedings of the conference "Nanomaterials by Severe Plastic Deformation, NANOSPD2", December 9-13, 2002, Vienna Austria*. Michael Zehetbauer and Ruslan Z. Valiev, edited by. Weinheim, Cambridge: Wiley-VCH; 2004.
[21] Song H-HG, Rumma RT, Ozaki CK, et al. Vascular tissue engineering: progress, challenges, and clinical promise. Cell Stem Cell. 2018;22(3):340–354.